

## Fast Flow Studies of Atomic Carbon Kinetics at Room Temperature

G. Dorthe,\* Ph. Caubet, Th. Vias, B. Barrère, and J. Marchais

*Laboratoire de Photophysique et Photochimie Moléculaire, Associé au C.N.R.S. No. 348, Université de Bordeaux I, 33405 Talence, France (Received: March 19, 1990; In Final Form: February 12, 1991)*

The reactions of atomic carbon with OCS, NO, O<sub>2</sub>, N<sub>2</sub>O, SO<sub>2</sub>, and H<sub>2</sub>S were studied at room temperature in a fast-flow reactor. The atomic carbon, which was obtained from the microwave dissociation of CO diluted in He, was homogeneously mixed with the reactant molecules in a section of flow tube far from the discharge. The pseudo-first-order decay of atomic carbon was determined from the decay of CS ultraviolet chemiluminescence produced by the C + OCS reaction. As electronically excited CS is rather long-lived, it is shown how long-lived chemiluminescence can be used for obtaining kinetic data. In flow experiments, the rigorous determination of pseudo-first-order reaction rate constants is given by solving the differential continuity equation of the decaying reactive species in the flow. However, in most studies such an effort is not undertaken and rate constants are determined assuming plug flow for the reactive species because it allows an easy conversion of decay distances into reaction times. In the present study both approaches have been used. The plug-flow rate constant values were found to be significantly smaller than those given by the solution of the continuity equation. Our study thus provides a new example of the danger of the plug-flow approximation when conditions justifying it are not fulfilled. Specifically, the plug-flow assumption requires low homogeneous and wall-depletion rates of the reactive species with respect to its diffusion rate in the carrier gas. In our experiments none of these conditions was fulfilled and, in particular, the atomic carbon wall removal was found to be very efficient. Rate constants were determined for the first time for the reactions with OCS, SO<sub>2</sub>, and H<sub>2</sub>S. For the reactions with O<sub>2</sub>, NO, and N<sub>2</sub>O, previous studies, essentially performed by flash photolysis, gave a large scatter of data. Our values do not match any of those data. However, agreement for relative rate coefficients is found with Husain's latest values, obtained at the lowest flash-lamp energy, which are furthermore the closest to ours. Our reaction rate constant values, given by the solution of the continuity equation of the atomic carbon in the flow, are (in 10<sup>-11</sup> cm<sup>3</sup> molecule<sup>-1</sup> s<sup>-1</sup> units): 10.1 ± 0.7 with OCS; 2.7 ± 0.2 with NO; 1.6 ± 0.2 with O<sub>2</sub>; 0.85 ± 0.16 with N<sub>2</sub>O; 6.9 ± 1.7 with SO<sub>2</sub>; and 8.3 ± 1.8 with H<sub>2</sub>S.

## Introduction

Only a few kinetic data concerning the reactivity of atomic carbon are available. Besides an early study in which the C + O<sub>2</sub> reaction rate constant at room temperature was estimated by a flow technique,<sup>1</sup> there have been four reports of carbon-atom kinetics, each studied at room temperature by flash photolysis. In the first three studies,<sup>2–4</sup> atomic carbon was produced by the vacuum ultraviolet photolysis of C<sub>3</sub>O<sub>2</sub> with a flash lamp and in the fourth<sup>5</sup> by the 248-nm excimer-laser photolysis of CH<sub>2</sub>Br<sub>2</sub>. In all of these experiments, only molecules believed to be largely unaffected by the photolyzing flash were added with the atomic carbon precursor molecule. In flash-lamp experiments, these were H<sub>2</sub>, N<sub>2</sub>, O<sub>2</sub>, NO, N<sub>2</sub>O, CO, CO<sub>2</sub>, CH<sub>4</sub>, C<sub>2</sub>H<sub>2</sub>, and C<sub>2</sub>H<sub>4</sub>, among which only O<sub>2</sub>, NO, and N<sub>2</sub>O were found to be reactive, NO being the most reactive and N<sub>2</sub>O the least. The determined rate constant values are in poor agreement. The recent laser-photolysis experiments were limited to NO and O<sub>2</sub>. In contradiction with the flash-lamp results, NO was found to be 3 times less reactive than O<sub>2</sub> (Table I). In addition, the value given by the earlier flow study of the C + O<sub>2</sub> reaction was 1 order of magnitude lower than any of the values given by the photolysis experiments. Based on these reports, no rate constant value could be assigned with confidence to the O<sub>2</sub>, NO, and N<sub>2</sub>O reactions. In addition, as pointed out above, the photolysis technique does not permit the study of carbon-atom reactions with photolyzable species such as OCS, SO<sub>2</sub>, and H<sub>2</sub>S—reactions that are very exoergic and liable to be fast at room temperature. This justifies our interest in a fast flow kinetic study of atomic carbon reactions with O<sub>2</sub>, NO, N<sub>2</sub>O, OCS, SO<sub>2</sub>, and H<sub>2</sub>S.

In the photolysis experiments, atomic carbon was monitored by either its resonance absorption at 165 nm<sup>2–4</sup> or its fluorescence

at 147 nm following its two-photon laser excitation at 287 nm.<sup>5</sup> For the present work we have developed a chemiluminescence method instead. We have previously shown that in an H + CHBr<sub>3</sub> + OCS diffusion flame at 300 K where atomic carbon C can only be produced in its ground state 2<sup>3</sup>P<sub>J</sub> (by H + CH → C + H<sub>2</sub>; H + CBr → C + HBr; or CH + CH → CH<sub>2</sub> + C), CS displays an intense chemiluminescence in the ultraviolet (a<sup>3</sup>π<sub>r</sub> → X<sup>1</sup>Σ<sup>+</sup>) transition. This chemiluminescence is ascribed to the spin allowed pathway C (2<sup>3</sup>P<sub>J</sub>) + OCS (X<sup>1</sup>Σ<sup>+</sup>) → CS (a<sup>3</sup>π<sub>r</sub>) + CO (X<sup>1</sup>Σ<sup>+</sup>).<sup>6</sup> Production of CS (a<sup>3</sup>π<sub>r</sub>) from reactive collisions between ground-state carbon atoms and carbonyl sulfide molecules has been recently confirmed in our crossed, pulsed, supersonic beam apparatus.<sup>7</sup> It is thus possible to correlate the CS chemiluminescence decay with the decay of ground-state atomic carbon in flow experiments.

For OCS alone in the presence of C, the rate constant of the C + OCS reaction was determined. When atomic carbon reacted with OCS + X mixtures (X ≡ O<sub>2</sub>, NO, N<sub>2</sub>O, SO<sub>2</sub>, H<sub>2</sub>S), the rate constants of several C + X reactions could also be determined.

## Experimental Section

Special attention was paid to the mixing of reactants and to the precision attached to the measurements of distances and chemiluminescence intensities.

A Teflon reaction tube, 36 mm inner diameter, was chosen to minimize the atomic carbon wall removal and the friction of the reactant mixing device (Figure 1) which slid smoothly inside. A 1 × 17 mm slit, facing a quartz window, was drilled in the tube for the observation of the chemiluminescence. Helium flowed between the slit and the window to avoid carbonaceous deposits on the window. Atomic carbon was produced by the microwave dissociation (75 W) of CO diluted in 2 Torr of He with the model I cavity designed by Vidal and Dupret.<sup>8</sup> The distance between the discharge and the reactant mixing device was held constant (27 cm). The design of the mixing device was chosen in separate

(1) Martinotti, F. F.; Welch, M. J.; Wolf, A. P. *J. Chem. Soc., Chem. Commun.* **1968**, 115.

(2) Braun, W.; Bass, A. M.; Davis, D. D.; Simmons, J. D. *Proc. R. Soc.* **1969**, *A312*, 417.

(3) Husain, D.; Kirsch, L. J. *Trans. Faraday Soc.* **1971**, *67*, 2025.

(4) Husain, D.; Young, A. N. *J. Chem. Soc., Faraday Trans. 2* **1975**, *71*, 525.

(5) Becker, K. H.; Brockmann, K. J.; Wiesen, P. *J. Chem. Soc., Faraday Trans. 2* **1988**, *84*, 455.

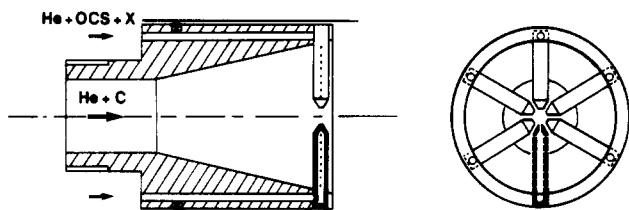
(6) Dorthe, G.; Caille, J.; Burdinski, S. *J. Chem. Phys.* **1983**, *78*, 594.

(7) Naulin, C.; Costes, M.; Dorthe, G.; Caubet, Ph. *J. Chem. Soc., Faraday Trans.* **1990**, *86*, 887.

(8) Vidal, B.; Dupret, C. *J. Phys. E., Sci. Instrum.* **1976**, *66*, 998.

**TABLE I: Comparison of the Rate Constant Values, from Several Investigations, of the Bimolecular Removal of C ( $2^3P_1$ ) by  $O_2$ , NO, and  $N_2O$  at Room Temperature (in  $10^{-11} \text{ cm}^3 \text{ molecule}^{-1} \text{ s}^{-1}$ )**

reactions	flow tube	flash-lamp photolysis			laser photolysis	flow tube
	ref 1	ref 2	ref 3	ref 4	ref 5	present work
C + $O_2$	$\approx 0.25$	$\approx 3.3$	$3.5 \pm 1.5$	$2.6 \pm 0.3$	$4.7 \pm 0.3$	$1.6 \pm 0.2$
C + NO		11.0	$7.3 \pm 2.2$	$4.8 \pm 0.8$	$1.6 \pm 0.2$	$2.7 \pm 0.2$
C + $N_2O$			$2.5 \pm 1.6$	$1.3 \pm 0.3$		$0.85 \pm 0.16$
ratios						
C + NO/C + $O_2$		3.3	2.1	1.8	0.3	1.7
C + $N_2O$ /C + $O_2$			0.7	0.5		0.5

**Figure 1.** Reactant mixing device sliding in the Teflon flow tube. The pinhole diameter is 0.3 mm.

experiments. The mixing pattern was first visually established by observing the green  $C_2$  chemiluminescence resulting from mixing of atomic hydrogen diluted in helium with  $CHBr_3$  also diluted in helium.<sup>9</sup> No striations could be observed. Homogeneous mixing of the reactants was thus quickly achieved, earlier than the establishment of the carrier gas parabolic velocity profile. Between the establishment of the velocity profile, estimated at 5 cm from the reactant mixing point and the end of the detectable chemiluminescence zone, at 10–12 cm, only a few centimeters were left for the decay measurements. The greatest precision available was thus required for the measurements of both the chemiluminescence intensities and the distances. The mixing device was slid along the Teflon tube with a stepper motor driven by a microcomputer. Each distance between the pinholes of the mixing device and the axis of the observation was obtained with a precision of 0.05 mm, as verified with a micrometer vernier for both forward and backward motions. For distance increments of 1 mm the average of 50 successive intensity measurements was recorded at each distance. With a clean quartz discharge tube and clean Teflon reactor tube, the chemiluminescence signal decreased to a stabilized value within 1 h. At that time the carbonaceous coatings of the two tubes resulted in stabilized efficiencies for the atomic carbon generation and its further wall removal. The chemiluminescence spectrum was recorded with a 0.6-m monochromator (Jobin Yvon HRS 1), the scanning of which was controlled by a microcomputer (IBM-PC). The photomultiplier (HTV R 955) output current was amplified (Keithley 427) and transferred to the microcomputer for storage and analysis. Gas pumping was achieved by a Roots blower (Edwards EH 500) backed by a mechanical pump (Alcatel EM 60). All flow rates were adjusted with thermal mass flowmeters and controllers (Tylan). The total pressure in the tube was measured along the axis of the tube with a capacitance manometer (Datametrics) having a range of 10 Torr full scale. The gases were used directly from the cylinders without further purification ( $He \geq 99.9995\%$ ,  $CO \geq 99.997\%$ ,  $OCS > 99.998\%$ ).

### Fast Flow Kinetics

For bimolecular reactions the pseudo-first-order rate constant of the reaction is usually determined from the axial decay of one reactant, the other being constant since it is in great excess. Such a rate constant is obtained by solving the differential continuity equation for the minor reactant concentration in the flow. However, as such a solving presents some difficulty, the extremely simple plug-flow approximation is commonly used instead. As our study provides a further example of the danger of such an

approximation in flow experiments,<sup>10</sup> we recall briefly these two possibilities.

**1. Continuity Equation.** The axial and radial distribution of a reaction species diluted in an inert carrier gas depends on the relative importance of convection by the carrier gas, removal by homogeneous reaction, removal at the wall, and diffusion within the carrier gas induced by axial and radial concentration gradients. All these contributions are included in the differential continuity equation for the reactive species in the flow, which can be expressed as<sup>11</sup>

$$\frac{\partial^2 C}{\partial y^2} + \frac{1}{y} \frac{\partial C}{\partial y} + \frac{\partial^2 C}{\partial x^2} - Pe f(y) \frac{\partial C}{\partial x} - aC = 0 \quad (1)$$

where  $C \equiv C(x, y)$  is the reactive species concentration;  $x = dR^{-1}$  is the reduced axial coordinate,  $d$  being the axial coordinate and  $R$  the tube radius;  $y = rR^{-1}$  is the reduced radial coordinate;  $a = R^2 k^{(1)}/D$ , where  $k^{(1)}$  is the pseudo-first-order reaction rate constant and  $D$  the binary diffusion coefficient of the reactive species in the carrier gas; and  $Pe = \langle u \rangle R/D$ , where  $\langle u \rangle$  is the mean axial flow velocity of carrier gas such that the radial dependence of the axial flow velocity is expressed as  $u(y) = \langle u \rangle f(y)$ , where  $f(y)$  is the carrier gas velocity profile;  $f(y) = 2(1 - y^2)$  for a fully developed steady parabolic velocity profile. The boundary conditions are

$$\text{on the axis:} \quad \partial C / \partial y = 0; \quad y = 0$$

$$\text{at the wall:} \quad \partial C / \partial y + bC = 0; \quad y = 1$$

$b = Rk_w/D$ , where  $k_w$  is the rate of wall removal along the radial coordinate  $y$ . It is expressed in  $\text{cm s}^{-1}$ .  $k_w = \gamma \langle c \rangle / 4$ , where  $\gamma$  is the wall sticking coefficient of the reactive species and  $\langle c \rangle$  its mean thermal velocity.

**2. The Plug-Flow Approximation.** The plug-flow approximation assumes that at any radial and axial coordinate set the reactant has the same axial velocity  $u_R$  equal to the mean axial carrier gas velocity  $\langle u \rangle$ . The axial reactant decay is related to the pseudo-first-order rate constant through the relationship:

$$-u_R dC/dz = kC + k_{wp} \quad (2)$$

or

$$-dC/dt = kC + k_{wp} \quad \text{as} \quad u_R = dz/dt \quad (3)$$

In such an approximation the first-order wall removal rate constant  $k_{wp}$  is expressed in  $\text{s}^{-1}$  and should not be confused with its corresponding term  $k_w$ , expressed in  $\text{cm s}^{-1}$ , in the boundary conditions of the continuity equation. The validity of the plug-flow approximation has been thoroughly discussed in many papers.<sup>10–16</sup>

(10) Howard, C. J. *J. Phys. Chem.* **1979**, *83*, 3.

(11) Lédé, J.; Villiermaux, J. *J. Chim. Phys.* **1977**, *74*, 459 (in French).

(12) Ferguson, E. E.; Fehsenfeld, F. C.; Schmeltekopf, A. *Adv. At. Mol. Phys.* **1969**, *5*, 1.

(13) Fontijn, A.; Felder, W. High Temperature Flow Tubes. Generation and Measurement of Refractory Species. In *Reactive Intermediates in the Gas Phase*; Setser, D. W., Ed.; Academic Press: New York, 1979.

(14) Hoyermann, K. H. Interactions of Chemical Reactions, Transport Processes and Flow. In *Physical Chemistry, an Advanced Treatise*; Jost, W., Ed.; Academic Press: New York, 1975; Vol. VIB.

(15) Brown, R. L. *J. Res. Natl. Bur. Stand.* **1978**, *83*, 1.

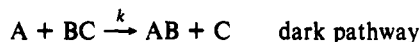
(16) Kaufman, F. *J. Phys. Chem.* **1984**, *88*, 4909.

(9) Arnold, S. J.; Kimbell, G. H.; Snelling, D. R. *Can. J. Chem.* **1975**, *53*, 2419.

The plug-flow approximation has the advantage that a given axial distance corresponds to a uniform reactant residence time, which is also the reaction time. The underestimation of the rate constant value given by this approximation increases with the rates for homogeneous and wall removal of the reactive species. In other words, when applying the plug-flow approximation one must expect a significant underestimation when both the apparent plug-flow values for the pseudo-first-order homogeneous removal rate and the wall first-order rate are large. In such a case, it is worth directly determining the pseudo-first-order homogeneous rate constant from the differential continuity equation of the reactive species in the flow since simple corrections to the plug flow results cannot be evaluated.

**3. On the Use of Chemiluminescence as a Reactant Tracer.** In our experiments we did not follow the reactant decay but the C + OCS chemiluminescence intensity. As a rule it is well-known that, for short-lived excited species, the steady-state approximation applies to the excited species concentration. Chemiluminescence intensity is proportional to reactant concentration since the very beginning of the reaction. Nevertheless, for long-lived species, for which such an approximation in its classical form does not apply, chemiluminescence decays can still be used to determine the reaction pseudo-first-order rate constant. Because this point may not be evident, it needs some clarification.

An homogeneous reaction involving a chemiluminescent pathway can be described by the following mechanism:



The excited species concentration is given by the relationship

$$[AB^*] = \frac{k^*[BC]}{k_e + k_q[M] - k_R[BC]} [A]_0 \exp(-k_R[BC]t) - \exp[-(k_e + k_q[M])t]$$

where  $k_R = k + k^*$  is the overall bimolecular reaction rate. This expression can be rewritten as

$$[AB^*] = \frac{k^*[BC]}{k_e + k_q[M] - k_R[BC]} [A]_0 \{1 - \exp[-(k_e + k_q[M] - k_R[BC])t]\} \exp(-k_R[BC]t) \quad (4)$$

since  $[A] = [A]_0 \exp(-k_R[BC]t)$ , (4) can be rewritten as

$$[AB^*] = \alpha [A] \{1 - \exp[-(k_e + k_q[M] - k_R[BC])t]\} \quad (5)$$

with

$$\alpha = \frac{k^*[BC]}{k_e + k_q[M] - k_R[BC]} \quad (6)$$

$[AB^*]$  reaches its maximum at a time  $t_M$  given by the relationship

$$t_M = \frac{\ln \{(k_e + k_q[M]) / k_R[BC]\}}{k_e + k_q[M] - k_R[BC]} \quad (7)$$

As a rule  $(k_e + k_q[M])$  exceeds  $k_R[BC]$  so that the excited species decay asymptotically becomes monoexponential with the decay constant  $k_R[BC]$ . To clear up the ideas, we present two realistic examples where we give the time for maximum intensity to be reached and the time  $t_c$  for which  $[AB^*] = 0.99\alpha[A]$  in order that the decay curve, approximated to a monoexponential decay from that time, should give a value of  $k_R[BC]$  underestimated by 1%. We present also the monoexponential decay given by the classical steady-state approximation:

$$[AB^*] = \frac{k^*}{k_e + k_q[M]} [A] \quad (8)$$

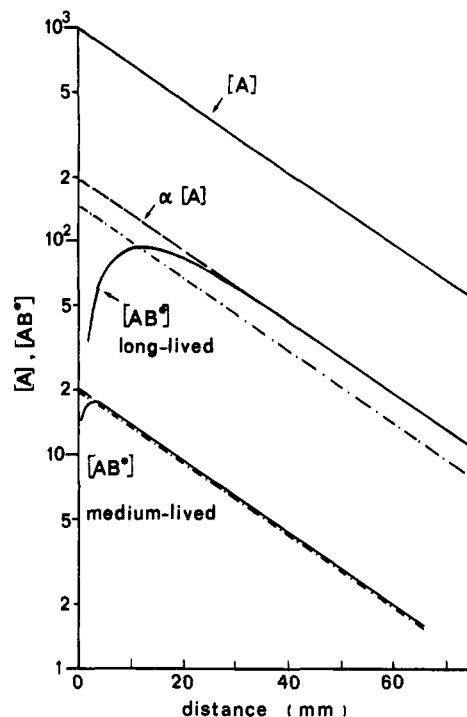


**Figure 2.** Decays of reactant and associated chemiluminescent excited species, arranged by the lifetime of the latter, in a chemiluminescence reaction. Chosen rate constant and lifetime values are given in text. The mixed dotted and interrupted line corresponds to the excited species decay as given by the classical steady-state approximation.

Times have been converted into distances for a reactant plug flow at a velocity  $u_R = 25 \text{ m s}^{-1}$ . The pseudo-first-order reaction rate constant has been taken as  $k_R[BC] = 1000 \text{ s}^{-1}$  and that for excited species production has been taken as  $k^*[BC] = 600 \text{ s}^{-1}$ . The latter value, which is rather high, has been chosen arbitrarily to give  $[A]$  and  $[AB^*]$  decay plots in the same figure (Figure 2). The collisional deactivation rate constant has been taken as  $k_q[M] = 4000 \text{ s}^{-1}$ . The first case corresponds to a long-lived species so that  $k_e$  is negligible with respect to  $k_q[M]$ ; for example,  $k_e = 63 \text{ s}^{-1}$  ( $\tau = 16 \text{ ms}$ ) for  $\text{CS}(a^3\pi_r)_{v=0}$ .<sup>17</sup> The maximum intensity is reached at a distance  $d_M = u_R t_M = 11.5 \text{ mm}$  where reactant concentration is 65% of its initial value. The critical distance for which  $[AB^*] = 0.99\alpha[A]$  is 38 mm. At such a distance, the reactant concentration has dropped to 20% of its initial value. The classical steady-state approximation does not fit asymptotic decay. For a medium-lived species such as  $k_e = 26 \times 10^3 \text{ s}^{-1}$  (so that  $\tau = 38 \text{ }\mu\text{s}$ ) the distances are shortened respectively to  $d_M = 2.7 \text{ mm}$  and  $d_c = 3.9 \text{ mm}$ . The classical steady-state approximation gives closer agreement with the actual asymptotic decay.

It is thus demonstrated that, despite the fact that the usual steady-state approximation does not apply for long-lived excited species, their asymptotic decay can still be used for the determination of reaction rate constants. Such kinetics equations have been described in terms of the reaction time. In the plug-flow approximation, the reactant axial residence time corresponds to the reaction time and the conversion from reaction time to distance is thus easily made. In the real case, the continuity equation does not allow such an explicitly defined reaction time.

The continuity equation can be solved through particular solutions of the type

$$C(x,y) \equiv [A]_{x,y} = g(y) \exp(-\lambda x) \quad (9)$$

The experimentalist, as a rule, is measuring a mean reactant concentration over a flow section at a given distance, so that experimental values refer to

$$\langle [A]_x \rangle = \langle g(y) \rangle \exp(-\lambda x) \quad (10)$$

(17) Black, G.; Sharpless, R. L.; Slinger, T. G. *J. Chem. Phys.* 1977, 66, 2113.

**TABLE II: Minimum Distance for a Fully Developed Parabolic Velocity Profile of the Carrier Gas under Our Experimental Conditions**

mean axial flow velocity ( $\mu$ ), m s <sup>-1</sup>	20	22.36	28.77
Reynolds number	15.75	17.60	22.77
$d_p = 0.228\text{Re}R$ , mm (refs 12, 13)	65	73	93
$d_p = 0.116\text{Re}R$ , mm (ref 14)	33	37	48
$d_p = 0.125\text{Re}R$ , mm (ref 19)	36	40	51
$d_p = (2 + 0.070\text{Re})R$ , mm (ref 20)	56	58	65

At a given axial distance, the chemiluminescence intensity measurement, giving a mean value of the intensity over the viewed section, is proportional to the mean excited CS concentration. The reactant flow can be decomposed as parallel concentric elementary plug flows. The distance for which

$$[AB^*]_{x,y} = 0.99\alpha[A]_{x,y} = 0.99\alpha g(y) \exp(-\lambda x)$$

will be dependent on radial coordinate  $y$ . Conversely, at a given axial distance, the proportionality constant between local excited species and reactant concentration will vary with the radial coordinate. However, if the axial distance is taken as the proportionality constant between  $[AB^*]_{x,y}$  and  $[A]_{x,y}$  varies between  $0.99\alpha$  and  $\alpha$ , we can assume  $[AB^*]_{x,y} \approx \alpha[A]_{x,y}$  over the whole tube section. In that case the mean excited species density can be assumed as proportional to the mean reactant density  $\langle [AB^*]_x \rangle = \alpha \langle [A]_x \rangle$ .

**4. Parabolic Velocity Profile of the Carrier Gas.** The solving of the differential continuity equation is undertaken for distances where the carrier gas has fully developed a steady parabolic profile. Rigorously, such a profile is asymptotic at infinite distance independent of the initial profile. The problem is thus to estimate at which distance the parabolic profile can be considered as reasonably well established. Theoretical distances have been proposed by different authors who assumed an initial plug-flow profile. Such an initial profile can be obtained experimentally by the turbulent introduction of a molecular reactant through a multihole array into the main carrier gas flow.<sup>12</sup> Such a distance  $d_p$  is given in terms of the Reynolds number  $\text{Re}$  of the flow and the radius of the tubular duct  $R$ . In review articles Ferguson et al.<sup>12</sup> and Fontijn and Felder<sup>13</sup> have referred to the same expression:  $d_p = 0.228\text{Re}R$ . In a recent article, Abbatt et al.<sup>18</sup> measured velocity profiles at 10.4 m from the gas injection in a tube whose inner radius was 61.8 mm. At such a distance the maximum  $\text{Re}$  value to observe the parabolic profile should be 700 as given by this relationship. However, the experimental profile was found to be nearly parabolic for Reynolds numbers varying from 1500 to 2500 (for which  $d_p$  is calculated to be 21 and 35 m). It is seen that such an expression largely overestimates the distance from which the profile can be assumed as parabolic. The twice lower values proposed by either Hoyermann<sup>14</sup> ( $d_p = 0.116\text{Re}R$ ) or Gersh et al.<sup>19</sup> ( $d_p = 0.125\text{Re}R$ ) thus can be considered all the more correct as the latter has been experimentally verified by Gersh et al. To complete the review on this subject, we would like to point out a study by Lédé,<sup>20</sup> unfortunately not published. In his experiments, hydrogen atoms produced in the annular discharge between two coaxial tubes were introduced in a flow tube of the dimensions of the inner discharge tube. The initial annular velocity distribution was thus the contrary of parabolic. Without any preconception, he measured velocity profiles along the distance for Reynolds numbers between 20 and 180. Flow visualization was performed with illuminated small particles carried by water. Photographs of particle trajectories allowed him to determine, from exposure time, local flow velocities. An example of such velocity

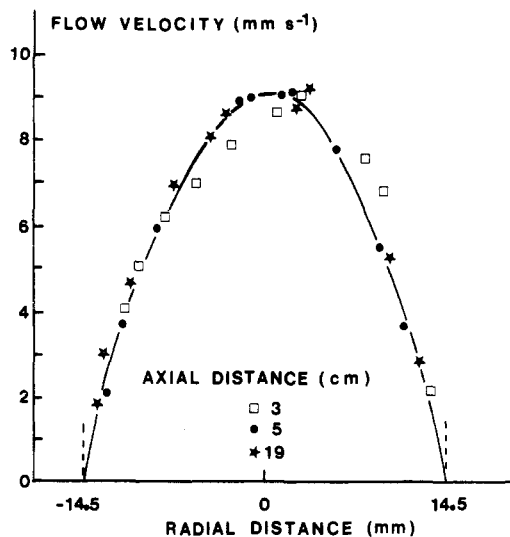
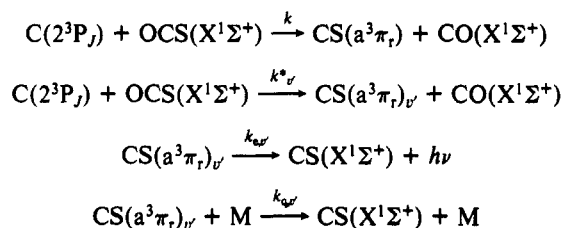


**Figure 3.** Variation of carrier gas velocity profile with the axial distance in a flow tube as determined by Lédé<sup>20</sup> (see text) for  $\text{Re} = 56$ . At 50 mm the parabolic profile is reached while his empirical formula gives 85 mm, showing that this formula gives a large security margin.

profiles is given in Figure 3. He deduced the empirical relationship for  $d_p$ :  $d_p = (2 + 0.070\text{Re})R$ . Under our conditions, the minimum distances given by the different relationships are in Table II. We thus conclude that for all our experiments a parabolic velocity profile can reasonably be assumed at a distance of 50 mm from the reactant mixing point. We started our decay measurements at that distance.

## Results

**1. CS Chemiluminescence.** The  $\text{CS}(a^3\pi_r \rightarrow X^1\Sigma^+)$  chemiluminescence spectrum from the  $\text{C} + \text{OCS} \rightarrow \text{CS} + \text{CO}$  reaction at 300 K has been previously published.<sup>6</sup> Vibronic bands, which range from 340 to 390 nm, do not overlap so that it was possible to follow their individual variation. Despite variations of 2 orders of magnitude for the absolute intensities of these bands along the flow axis, we could not observe any variation in their relative distribution. Thus, it can be concluded that vibrational relaxation within the  $\text{CS}(a^3\pi_r)$  state was negligible with respect to electronic quenching. The density of each vibrational level of this electronic state results from the balance between its production and its removal by spontaneous ultraviolet emission and collisional electronic quenching. The chemiluminescence reaction scheme can be represented as



Each vibronic excited state should asymptotically decay monoexponentially as does atomic carbon, verifying thus

$$[\text{CS}_{v'}] = \alpha_{v'}[\text{C}] \quad \text{with} \quad [\text{CS}^*] = \sum_{v'} \alpha_{v'}[\text{C}]$$

The decay of a vibronic level  $v'$  is given by the decay of any vibronic band ( $v' - v''$ ) whose intensity in arbitrary units is given by

$$I_{v'v''} = \beta_{v'v''}[\text{CS}_{v'}] \quad (11)$$

which asymptotically leads to

$$I_{v'v''} = \beta_{v'v''}\alpha_{v'}[\text{C}] \quad (12)$$

$\beta_{v'v''}$  is a constant including a geometrical factor, the detection efficiency, and the ( $v' - v''$ ) transition probability. We chose to

(18) Abbatt, J. P. D.; Demerjian, K. L.; Anderson, J. G. *J. Phys. Chem.* **1990**, *94*, 4566.

(19) Gersh, M. E.; Silver, J. A.; Zahniser, M. S.; Kolb, C. E.; Brown, R. B.; Gozewski, C. M.; Kalleis, S.; Wormhoudt, J. C. *Rev. Sci. Instrum.* **1981**, *52*, 1213.

(20) Lédé, J. Use of Flow Reactors for the Study of Coupled Elementary Diffusion and Reaction Processes, Involving very Reactive Species in the Gas Phase. Application to some Reactions of Atomic Hydrogen. Thesis, Nancy, December 1975 (in French).

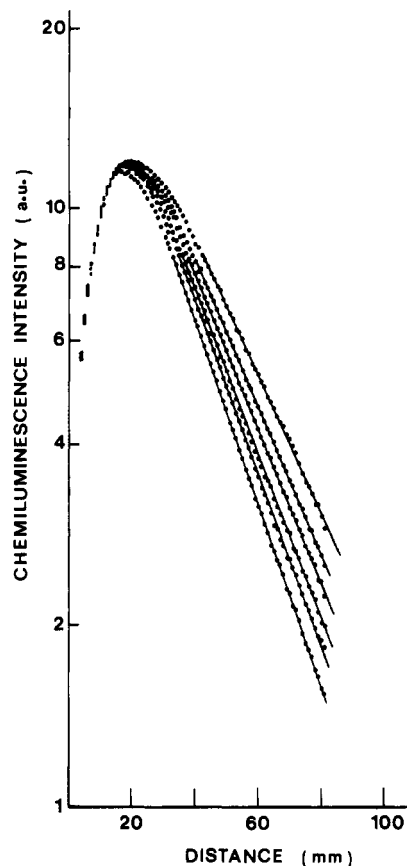


**Figure 4.** Example of CS chemiluminescence variation with the distance for a mean axial flow velocity ( $u$ ) of  $28.77 \text{ m s}^{-1}$  and a helium pressure of 2 Torr in a semilog plot. The slopes of the linear decays have been calculated from points at distances greater than 50 mm where the parabolic carrier gas profile may be ascertained. The successive OCS concentrations are (in  $10^{13} \text{ molecule cm}^{-3}$ ): 0.683; 0.775; 0.835; 0.911; 0.987; 1.078. The corresponding slopes (in  $\text{m}^{-1}$ ) with the 95% confidence interval  $t\sigma$  were found to be  $26.87 \pm 0.69$ ;  $28.87 \pm 0.73$ ;  $30.19 \pm 0.71$ ;  $31.90 \pm 0.85$ ;  $33.70 \pm 0.93$ ;  $35.49 \pm 0.90$ .

follow the decay of the (0-0) band because it is the most intense. Thus, for simplification, we shall skip any  $v'$  or  $v''$  subscript and our quenching rate constants will refer implicitly to  $v' = 0$ .

**2. C + OCS Reaction.** Lédé and Villermaux<sup>11</sup> pointed out that particular solutions of the continuity equation, as given by relationship 9, could be searched for, provided that the value of the dimensionless pseudo-first-order rate constant  $a$  does not exceed 30. For the extreme case of a gas kinetics value for the C + OCS bimolecular rate constant, this criterion gives  $10^{13} \text{ molecules cm}^{-3}$  as a maximum for the OCS concentration. [OCS] did not exceed such a value in our experiments.

Typical variations of CS chemiluminescence when OCS is added alone to the main stream of atomic carbon diluted in helium is given in Figure 4 for the highest flow velocity used. The distance for which chemiluminescence reaches a maximum is dependent on the OCS concentration. On Figure 4 it varies from 17 mm, for the greatest concentration, to 20 mm, for the lowest. These distances should not be confused with the distance needed to achieve mixing of reactants. It is due to the kinetics of production of CS ( $a^3\pi_r$ ) <sub>$v=0$</sub>  which is rather long-lived ( $\tau \approx 16 \text{ ms}$ )<sup>17</sup> because the  $a^3\pi_r \rightarrow X^1\Sigma^+$  transition is spin forbidden. It closely resembles the evolution given in Figure 2, modified by the mixing effect. Under the same conditions, the maximum intensity was observed at a shorter distance with chemiluminescences of short-lived species so that we can consider mixing as achieved within 10 mm. For distances greater than 50 mm the intensity decay can be considered as monoexponential for each OCS concentration involved, as verified by usual linearity tests (see below). When the OCS concentration is increased, the proportionality coefficient  $\alpha$  (relation 6) between  $[\text{CS}^*]_{v=0}$  and  $[\text{C}]$  exhibits a very weak variation from run to run. It can be explained by the fact that the numerator

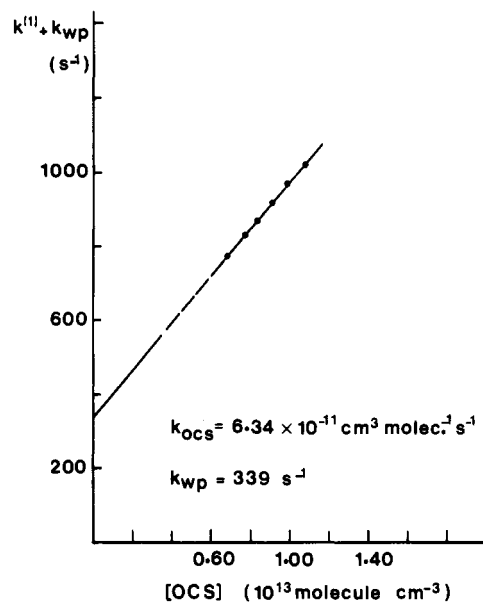


**Figure 5.** Plot of the overall plug-flow pseudo-first-order rate constant against [OCS] from experiments of Figure 4.

of  $\alpha$  is proportional to [OCS] while the denominator is almost proportional to [OCS]. This can be understood as quenching dominates over the spontaneous emission for the removal of the excited CS. Further, from known quenching rate constants,<sup>17,21</sup> the quenching term from OCS is much larger than the additional quenching terms from He and CO.

For each decay, the F linearity test<sup>22,23</sup> with  $n - 2$  and  $n(k - 1)$  degrees of freedom was applied to the semilog plot of experimental decay from a distance of 50 mm. Here  $n$  corresponds to the number of different distance values greater than 50 mm ( $n_{\text{max}} = 35$ ), and  $k$  is the number of intensity measurements at a given distance ( $k = 50$ ). The hypothesis of linearity for the semilog decay plot has been verified with a probability of 95%. Estimates of the linear parameters (slope and ordinate at the origin) of the semilog plot were obtained through the least-squares method. However, the estimates thus found may not minimize the sum of the squares of the residuals between experimental data points and their assumed monoexponential decay. Thus, estimates from semilog plots must be improved by taking into account the influence of the linearization transformation from the monoexponential form to the semilog linear form.<sup>24</sup> The so-called "improved" parameters were actually found identical with the former.

Each decay slope yielded a value of  $k_{\text{OCS}}[\text{OCS}] + k_{\text{wp}}$ , in the plug-flow approximation. Plotting these values against [OCS] (Figure 5) gave  $k_{\text{OCS}} = 6.3 \times 10^{-11} \text{ cm}^3 \text{ molecule}^{-1} \text{ s}^{-1}$  and  $k_{\text{wp}} = 339 \text{ s}^{-1}$ . Owing to these large values, the validity of the plug-flow approximation could be questioned. We thus tackled the problem of solving the continuity equation for atomic carbon in the flow.

To determine  $k^{(1)}$  from a measured  $\lambda$  value, the values of  $D_{\text{C-He}}$  and  $k_w$  are needed. Unfortunately, we found none in the literature. The value of  $D_{\text{C-He}}$  can be estimated by comparison with that of  $D_{\text{O-He}}$ . However, there is no way to estimate  $k_w$  so that, for the estimated  $D_{\text{C-He}}$  value, the calculated  $k^{(1)}$  value from one decay will depend on the arbitrary value given to  $k_w$ . Fortunately, this dependence must be weak for  $\lambda(u)R/D \geq 5$ ,<sup>11</sup> as is the case in our experiments. Anyway, the correct  $k_w$  value was found by using the self-consistency condition that, for OCS alone as a reactant,  $k^{(1)} = k_{\text{OCS}}[\text{OCS}]$  should be proportional to [OCS]. The coef-

(21) Taylor, G. W. *J. Phys. Chem.* **1973**, *77*, 124.

(22) Bowker, A. H.; Lieberman, G. J. *Engineering Statistics*; Prentice-Hall: New York, 1959.

(23) Bevington, P. R. *Data Reduction and Error Analysis for the Physical Sciences*; McGraw-Hill: New York, 1969.

(24) Aivazian, S. *Etude Statistique des Dependances*; Editions Mir: Moscow, 1978.

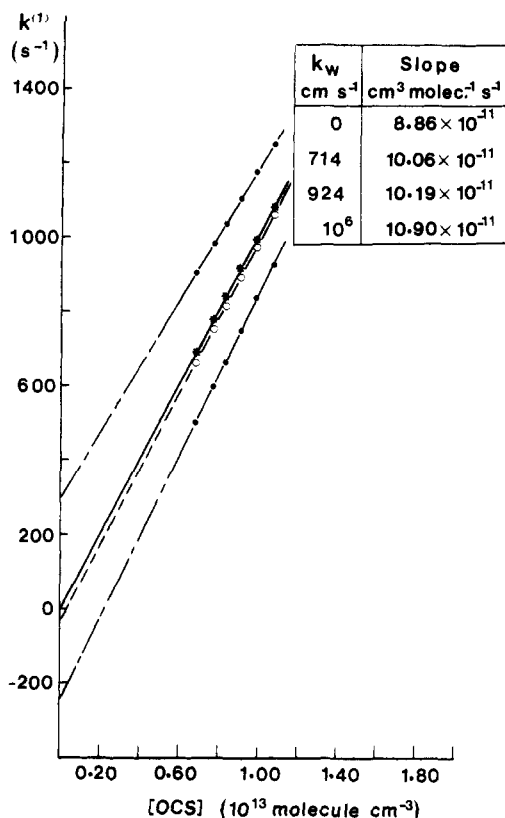


**Figure 6.** Plot of the pseudo-first-order rate constant against [OCS] given by the resolution of the differential continuity equation. The binary diffusion coefficient was taken as  $D_{C-He} = 430 \text{ cm}^2 \text{ s}^{-1}$ . The wall removal coefficient  $k_w$  being unknown, several trials were made, the correct one being at  $714 \text{ cm s}^{-1}$  which gives the proportionality of  $k^{(1)}$  with OCS. The mean value of  $k_w$  in our experiments was  $924 \text{ cm s}^{-1}$ .

ficient  $D_{A-B}$  (in  $\text{cm}^2 \text{ s}^{-1}$ ) for diffusion of an atomic species A in an other atomic species B at a given absolute temperature  $T$  and a given total pressure  $P$  (in Torr) can be calculated according to the relationship<sup>25</sup>

$$D_{A-B} = \frac{8}{P(\sigma_A + \sigma_B)^2} \left[ T^3 \frac{(M_A + M_B)}{2M_A M_B} \right]^{1/2} \quad (13)$$

where  $\sigma_A$  and  $\sigma_B$  are the collision diameters (in Å) of atomic species A and B for A + B collisions,  $M_A$  and  $M_B$  being their atomic masses. Collision diameters of atomic nitrogen and atomic oxygen were found to be very close ( $\sigma_O = 2.65 \text{ Å}$  and  $\sigma_N = 2.75 \text{ Å}$ )<sup>26</sup> when determined by using the same experimental technique. Since  $\sigma_N \approx \sigma_O$  we further assumed  $\sigma_C \approx \sigma_N \approx \sigma_O$  so that we could determine  $D_{C-He}$  from  $D_{O-He}$ , through the relationship 13. We chose  $D_{O-He}$  instead of  $D_{N-He}$  because measurements of  $D_{O-He}$  have been performed by different authors and techniques, which was unfortunately not the case for  $D_{N-He}$ . From four different determinations, Judeikis and Wun<sup>25</sup> propose as a mean value for  $D_{O-He}$ ,  $1.08 \pm 0.12 \text{ cm}^2 \text{ s}^{-1}$  at 760 Torr and for a temperature of 295 K. Thus from masses of atomic oxygen and atomic carbon we deduced  $D_{C-He} \approx 430 \pm 48 \text{ cm}^2 \text{ s}^{-1}$  at 2 Torr and for  $T = 298 \text{ K}$ . We used that value for the resolution of continuity equation.

By including in the continuity equation the  $\lambda$  decay values from Figure 4 and taking  $k_w = 714 \text{ cm s}^{-1}$  we obtained for each [OCS] value a pseudo-first-order rate constant  $k^{(1)} = k_{OCS}[OCS]$ . This choice of the  $k_w$  value is based on which  $k^{(1)}$  was found proportional to [OCS] as shown in Figure 6. From the slope of the linear plot of  $k^{(1)}$  against [OCS] we found  $k_{OCS} = 10.06 \times 10^{-11} \text{ cm}^3 \text{ molecule}^{-1} \text{ s}^{-1}$  with a standard deviation  $\sigma$  of  $0.66 \times 10^{-11} \text{ cm}^3 \text{ molecule}^{-1} \text{ s}^{-1}$  and a 95% confidence limit  $t\sigma$  of  $1.46 \times 10^{-11} \text{ cm}^3$

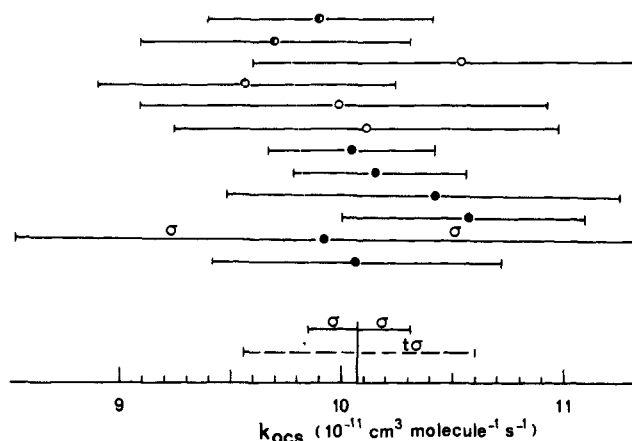


**Figure 7.** Distribution of rate constant values for the C + OCS reaction for six experiments at a mean axial flow velocity ( $u$ ) of  $28.77 \text{ m s}^{-1}$  (solid circles), two at a velocity ( $u$ ) of  $22.75 \text{ m s}^{-1}$  (half solid circles), and four at a velocity ( $u$ ) of  $20 \text{ m s}^{-1}$  (open circles). Standard deviations  $\sigma$  are given for each experiment and the 95% confidence interval  $t\sigma$  for the average value  $k_{OCS} = (10.08 \pm 0.52) \times 10^{-11} \text{ cm}^3 \text{ molecule}^{-1} \text{ s}^{-1}$  for  $D_{C-He} = 430 \text{ cm}^2 \text{ s}^{-1}$ . Using  $D_{C-He} = 385 \text{ cm}^2 \text{ s}^{-1}$  gives a shift of  $+0.2 \times 10^{-11} \text{ cm}^3 \text{ molecule}^{-1} \text{ s}^{-1}$  and using  $D_{C-He} = 475 \text{ cm}^2 \text{ s}^{-1}$  gives a shift of  $-0.2 \times 10^{-11} \text{ cm}^3 \text{ molecule}^{-1} \text{ s}^{-1}$  for the  $k_{OCS}$  value.

$\text{molecule}^{-1} \text{ s}^{-1}$ . This value is 1.6 times greater than the plug-flow value. To reduce the uncertainty ranges defined by  $\sigma$  and  $t\sigma$ , 12 determinations of  $k_{OCS}$  were made, six at a velocity ( $u$ ) of  $28.77 \text{ m s}^{-1}$ , four at a velocity ( $u$ ) of  $20.00 \text{ m s}^{-1}$ , and two at a velocity ( $u$ ) of  $22.36 \text{ m s}^{-1}$ . They are summed up in Figure 7. We obtained  $k_{OCS} = 10.08 \times 10^{-11} \text{ cm}^3 \text{ molecule}^{-1} \text{ s}^{-1}$  with a standard deviation  $\sigma$  of  $0.23 \times 10^{-11} \text{ cm}^3 \text{ molecule}^{-1}$  and a 95% confidence limit  $t\sigma$  of  $0.52 \times 10^{-11} \text{ cm}^3 \text{ molecule}^{-1} \text{ s}^{-1}$ . The above determinations were performed with an assumed value of the diffusion coefficient of atomic carbon in helium. A possible 10% systematic error for that value leads to a 2% systematic shift on the rate constant, the attached  $\sigma$  and  $t\sigma$  on both sides of the shifted rate constant being unchanged. The uncertainty ranges given by  $t\sigma$  should be thus increased by  $0.2 \times 10^{-11} \text{ cm}^3 \text{ molecule}^{-1} \text{ s}^{-1}$  corresponding to this possible systematic shift as an increase or a decrease of the rate constant. In conclusion, our experiments lead to

$$k_{OCS} = (10.1 \pm 0.7) \times 10^{-11} \text{ cm}^3 \text{ molecule}^{-1} \text{ s}^{-1}$$

This value is 1.6 times greater than that obtained from the plug-flow approximation, thus giving evidence that the latter is not justified under these experimental conditions.

**3. C + X (X  $\equiv$  NO, O<sub>2</sub>, N<sub>2</sub>O, SO<sub>2</sub>, H<sub>2</sub>S) Reactions.** In these experiments atomic carbon reacted with OCS + X. The OCS was, for all experiments, held at the same small concentration since its role was only to yield a chemiluminescence intensity proportional to the atomic carbon concentration. The pseudo-first-order rate constant  $k^{(1)} = k_{OCS}[OCS] + k_X[X]$  given by each chemiluminescence decay could be used to determine  $k_X$  from its variation with [X]. In these experiments, the proportionality coefficient  $\alpha$  (relation 6) between the excited species concentration and that of atomic carbon decreases from run to run for increasing [X] since its numerator is held constant while its denominator increases with [X] through the X quenching term. Such decays are exemplified for X  $\equiv$  NO in Figure 8. The plot of  $k^{(1)} + k_{wp}$  against [NO], in the plug-flow approximation yielded

$$k_{NO} = (1.69 \pm t\sigma = 0.21) \times 10^{-11} \text{ cm}^3 \text{ molecule}^{-1} \text{ s}^{-1} \quad (\text{Figure 9})$$

The values given by the resolution of the continuity equation are

$$k_{NO} = (2.70 \pm t\sigma = 0.34) \times 10^{-11} \text{ cm}^3 \text{ molecule}^{-1} \text{ s}^{-1} \quad (\text{Figure 10})$$

Here again the plug-flow approximation yielded too low a value so that it should not be mentioned again. Nine different deter-

(25) Judeikis, H. S.; Wun, M. *J. Chem. Phys.* **1978**, *68*, 4123.

(26) Morgan, J. E.; Schiff, H. I. *Can. J. Chem.* **1964**, *42*, 2300.

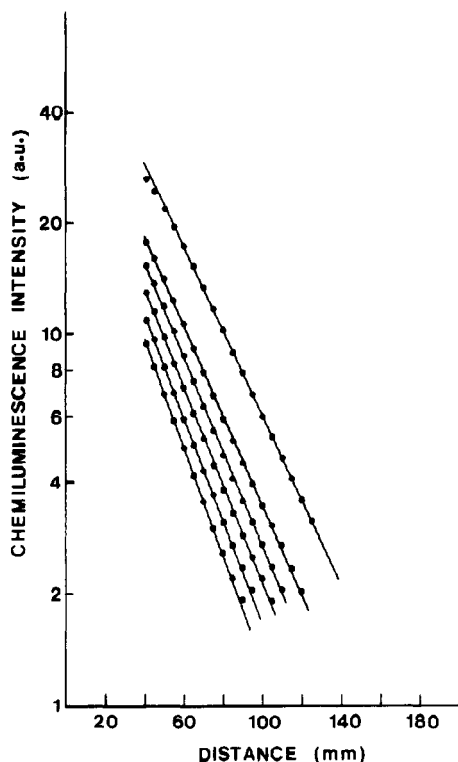


**Figure 8.** Example of CS chemiluminescence decays for a reactant mixture OCS + NO. For all decays  $[\text{OCS}] = 0.607 \times 10^{13}$  molecules  $\text{cm}^{-3}$ . The successive NO concentrations are (in  $10^{13}$  molecules  $\text{cm}^{-3}$ ) 0; 0.414; 0.620; 0.827; 1.039; 1.262. The corresponding slopes with the 95% confidence interval  $t\sigma$ , in the semilog plot, are in  $\text{m}^{-1}$ :  $26.45 \pm 0.17$ ;  $28.29 \pm 0.61$ ;  $30.19 \pm 0.40$ ;  $31.32 \pm 0.44$ ;  $32.30 \pm 0.38$ ;  $33.74 \pm 0.41$ . The mean axial flow velocity ( $u$ ) is  $28.77 \text{ m s}^{-1}$  under a 2 Torr of helium pressure.

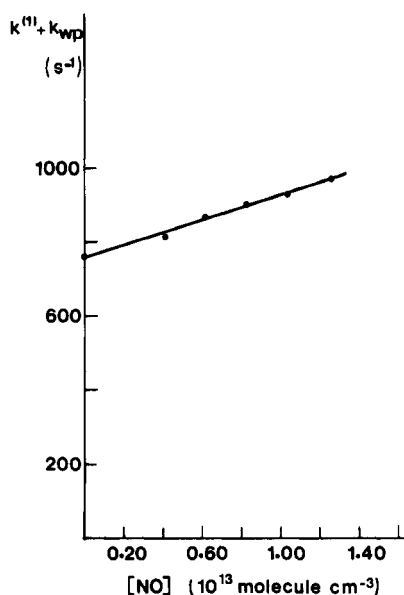


**Figure 9.** Plot of the plug-flow overall pseudo-first-order rate constant  $k^{(1)} + k_{wp} = k_{\text{OCS}}[\text{OCS}] + k_{\text{NO}}[\text{NO}]$  to  $k_{wp}$  as a function of  $[\text{NO}]$ , from the results of Figure 8.  $k_{\text{NO}} = (1.69 \pm t\sigma = 0.21) \times 10^{-11} \text{ cm}^3 \text{ molecule}^{-1} \text{ s}^{-1}$ .

minations were made at different flow velocities (Figure 11). Including the uncertainty on  $D_{\text{C-He}}$ , the rate constant was found to be

$$k_{\text{NO}} = (2.7 \pm 0.2) \times 10^{-11} \text{ cm}^3 \text{ molecule}^{-1} \text{ s}^{-1}$$

The same procedure was followed for  $X \equiv \text{O}_2$ ,  $\text{N}_2\text{O}$ ,  $\text{SO}_2$ , and  $\text{H}_2\text{S}$ . For  $\text{O}_2$  and  $\text{N}_2\text{O}$ , results are given in Table I. For  $\text{SO}_2$  and  $\text{H}_2\text{S}$ , the reaction rate constant expressed in  $10^{-11} \text{ cm}^3 \text{ molecule}^{-1} \text{ s}^{-1}$

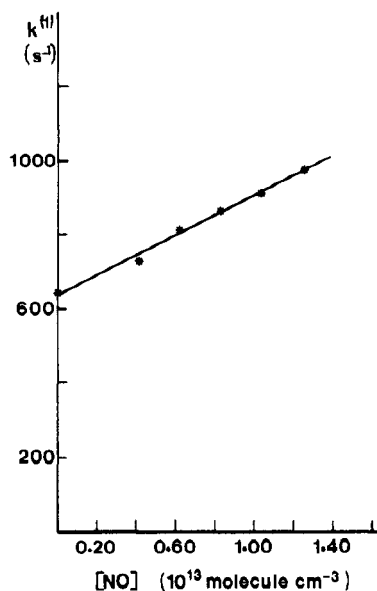


**Figure 10.** Plot of the pseudo-first-order rate constant  $k^{(1)} = k_{\text{OCS}}[\text{OCS}] + k_{\text{NO}}[\text{NO}]$  as a function of  $[\text{NO}]$ , from the results of Figure 8,  $k^{(1)}$  being calculated by the resolution of the differential continuity equation.  $k_{\text{NO}}$  is found to be  $(2.70 \pm t\sigma = 0.34) \times 10^{-11} \text{ cm}^3 \text{ molecule}^{-1} \text{ s}^{-1}$ .

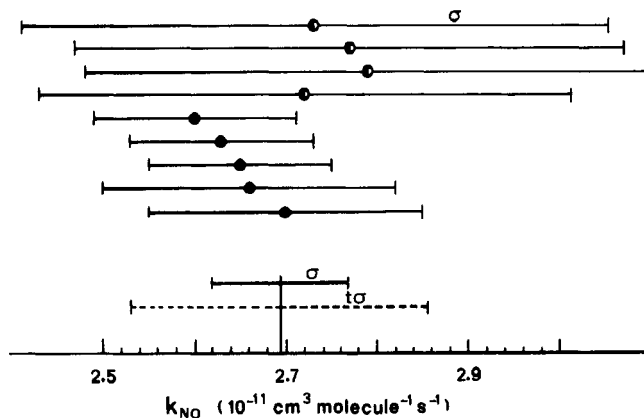


**Figure 11.** Successive rate constant  $k_{\text{NO}}$  determinations. The mean axial carrier gas velocity ( $u$ ) is  $28.77 \text{ m s}^{-1}$  (solid circles) and  $22.75 \text{ m s}^{-1}$  (half solid circles).

are found to be respectively  $6.9 \pm 1.7$  and  $8.3 \pm 1.8$ .

### Discussion

As shown in Table I, none of our data concerning  $\text{C} + \text{O}_2$  and  $\text{C} + \text{N}_2\text{O}$  agree with those found by previous investigations which are also in poor agreement with one another. Since we did not find agreement with absolute values, we checked the ratios of the rate constants (Table I). There we find agreement with the ratios obtained by Husain and Young. Their absolute values also are the closest to ours.

For clarity of discussion, we recall briefly the evolution of the successive rate constant values given in the three flash-lamp photolysis studies,<sup>2-4</sup> from the earliest by Braun et al.<sup>2</sup> to the most recent by Husain and Young. In these three studies, atomic carbon was generated from the vacuum-UV flash-lamp photolysis of  $\text{C}_3\text{O}_2$  and monitored through its resonant absorption at 165 nm. However, despite their basic similarities, those studies differ in the quality of experimental procedure. Braun et al. measured the atomic carbon concentration with a second flash lamp, in the presence of different reactant concentrations, at a fixed delay time of  $10 \mu\text{s}$  from the photolyzing flash by plate photometry. Husain and Kirsch<sup>3</sup> improved experiments by monitoring the whole decay of atomic carbon in single-shot experiments where the flash energy was 1125 J, with a continuous carbon resonance lamp and a photomultiplier. In a further study, Husain and Young were able to lower the flash energy to 180 J by averaging decays over 16

successive shots. They found lower rate constant values. They concluded that their latter lower values were to be preferred on account of smaller contributions to the decay of atomic carbon by products resulting from the photolysis of reactants. However, they did not say whether these contributions became negligible in these latest experiments and it is unfortunate that the rate constant values have not been extrapolated to a zero flash energy. Our results provide strong evidence for the presence of a photolytic interference in the flash-lamp experiments and suggest that the slightly larger values observed by Husain and Young are due to this effect.

We find no agreement, in any manner, with the laser photolysis experiments of Becker et al.<sup>3</sup> In their experiments, atomic carbon was generated from the multiphoton dissociation of CH<sub>2</sub>Br<sub>2</sub> at 248 nm, with the focused KrF radiation from an excimer laser. The radiation energy in the tiny focal volume of the laser is several orders of magnitude greater than in the large volume irradiated by a flash lamp. Husain and Young have demonstrated that C + NO and C + O<sub>2</sub> rate constants depend on the flash-lamp energy, providing evidence that such determinations were affected by the contribution of reactant photolysis products to the atomic carbon decay. Such a problem must be even greater in laser photolysis experiments since the photon-energy density allows multiphoton

processes to affect the reactants more severely and in a hard to predict way. Unfortunately, no information is given by Becker et al. about the influence of laser intensity on their atomic carbon decays.

Our experiments with O<sub>2</sub>, NO, and N<sub>2</sub>O allowed the contradictions between flash lamp and laser photolysis experiments to be cleared up.

#### Conclusion

The fast flow technique has allowed us to determine the rate constants of atomic carbon reactions with OCS, SO<sub>2</sub>, and H<sub>2</sub>S for the first time. For reactions with O<sub>2</sub>, NO, and N<sub>2</sub>O, where a rather large scatter of rate constant values had been given by either flash-lamp or laser-photolysis experiments, our results have been found to be close, but at a lower value, to those given by flash-lamp experiments at the lowest flash energy. More generally, our study provides a new example of the danger of significantly underestimating rate constant values when assuming plug flow in flow experiments combining fast homogeneous gas-phase reactions and efficient wall removal.

*Acknowledgment.* We thank C. Lalaude for technical assistance with the flow reactor.

## Mechanism of Photodegradation of Aqueous Organic Pollutants. 1. EPR Spin-Trapping Technique for the Determination of <sup>•</sup>OH Radical Rate Constants in the Photooxidation of Chlorophenols following the Photolysis of H<sub>2</sub>O<sub>2</sub>

Jan Kochany<sup>†</sup> and James R. Bolton\*

*Photochemistry Unit, Department of Chemistry, The University of Western Ontario, London, Ontario, Canada N6A 5B7 (Received: August 22, 1990; In Final Form: January 15, 1991)*

A technique for the determination of the rate constants for the reaction of <sup>•</sup>OH radicals with organic substrate is described. This technique is based on the use of spin trapping with electron paramagnetic resonance (EPR) detection of spin adducts. The desired rate constants are obtained by measuring either the initial rate of production of the EPR signal of the spin adduct or its amplitude after a fixed time, as a function of the concentration of the substrate. By using the known rate constant for the reaction of <sup>•</sup>OH radicals with the spin trap (DMPO), rate constants for the reaction of <sup>•</sup>OH radicals with a given substrate can be obtained within a competition kinetic scheme. The method has been validated by determining the rate constants for the reaction of <sup>•</sup>OH radicals with phenol and with formate, two reactions well studied by using pulse radiolysis. Our results agree with literature values within experimental error. The method is then applied to several chlorophenols. The rate constants for 3-chloro-substituted phenols are significantly less than for 4-chloro or 2-chloro-substituted phenols. Some rate constants are significantly larger than the diffusion-controlled rate constant. This is explained by proposing a Grotthus-type mechanism for the movement of <sup>•</sup>OH radicals through water.

#### Introduction

Most of the earth's surface is covered by water in the form of oceans, seas, rivers, lakes, and ponds. Many chemicals are entering the aquatic environment because of human activities, including chemical discharges from the production, processing, use, and disposal of industrial and agricultural products. The total amount of these discharges has increased dramatically during the last forty years and is now the subject of considerable concern regarding their impact on both the aquatic environment and human health.

Many organic chemicals discharged into the environment are not only toxic but also only partly biodegradable, in that they are not easily removed in biological wastewater treatment plants. That is why there is a need to develop effective methods for the degradation of organic pollutants, either to less harmful compounds or, more desirable, to their complete mineralization.

Lately a series of new techniques, called advanced oxidation processes, has received increasing attention. They rely on the use of short-lived oxidative radicals (often hydroxyl radicals) generated by photolysis or radiolysis.<sup>1-5</sup> In spite of several reports and reviews<sup>6-8</sup> reporting degradation rates for a variety of pollutants, very little is known about the detailed mechanism of these deg-

- (1) Koubek, E. *Ind. Eng. Chem. Process. Des. Dev.* **1975**, *14*, 348.
- (2) Malaiyandi, M.; Sadar, M. H.; Lee, P.; Grady, R. O. *Water Res.* **1980**, *14*, 1131.
- (3) Mansour, M. *Bull. Environ. Contam. Toxicol.* **1985**, *34*, 89.
- (4) Jacob, N.; Balakrishnan, I.; Reddy, M. P. *J. Phys. Chem.* **1977**, *81*, 17.
- (5) Prat, C.; Vicente, M.; Esplugas, S. *Water Res.* **1988**, *22*, 663.
- (6) Langford, C. H.; Carey, J. H. *ACS Symp. Ser.* **1987**, *327*, 225.
- (7) Ollis, D. F.; Pelizzetti, E.; Serpone, N. In *Photocatalysis, Fundamentals and Applications*; Serpone, N., Pelizzetti, E., Eds.; John Wiley: New York, 1989; Chapter 18.
- (8) Matthews, R. W. *J. Phys. Chem.* **1987**, *91*, 3328.

<sup>†</sup>On leave from the Institute for Environmental Protection, Warsaw, Poland.